

Influence of temperature changes on a linear motion system

Jonathan. Abir, Paul. Shore, Paul. Morantz
Cranfield University, UK

Abstract

This paper assess the thermal distortion due to environmental temperature changes of a linear motion system proposed for a novel 6 axes CNC machining system - $\mu 4$. Whilst the machine structure is aluminium based, the air bearing guideways are made of alumina with a significantly lower coefficient of thermal expansion and higher specific stiffness compared to aluminium.

A 'bimetallic' design was proposed to stiffen the structure and to achieve better static and dynamic performances. However, there is a potential of a significant thermal distortion. A "bottom up" method was used to measure and simulate the thermal distortion of the proposed design focusing on the linear guideways. A unique setup was developed to allow heating and measuring the components while mounted on a coordinate measuring machine. The study shows that design symmetry reduces significantly the thermal distortion by restraining it.

1 Introduction

The increasing demand within electro-optics and information technology industries for ultra-precise micro-mechanical components sets new demands for improved small sized production machines. Numerous research efforts to develop so-called "compact" size machines have been undertaken in the past two decades. The trend to scaling down the work-piece sizes requires higher precision machine accuracy and alignment of drive, bearing and measuring system. However, most of these machines are still at the development level and not been widely commercialised, moreover their application to high accuracy and fine surface quality is constrained by their low dynamic stiffness. The $\mu 4$ machine was conceived in 2008 [1] by Cranfield University Precision Engineering Institute. The machine was designed to allow both diamond turning and micro-milling with the ability to automatically shift operation mode

seamlessly. The overall size of the machine was set in the range of $0.6 \times 0.6 \times 1$ m. The machine is assembled by the following sub modules (Figure 1): frame, electronics cabinet, tool changer, XAC motion module axes and YDS motion module axes. In order to reduce assembly costs the machine design was based on common modules with simple interfaces. Thus, the machine motion axes were split into two near identical modules. Each module consists of two rotary and one linear motions made by direct drive motors. The YDS module is mounted on the vertical Z linear axis and the XAC module is held in a fixed position off the top of the machine structure. To avoid thermal asymmetry which can induce significant machine distortion, the machine design incorporates two axes of symmetry.

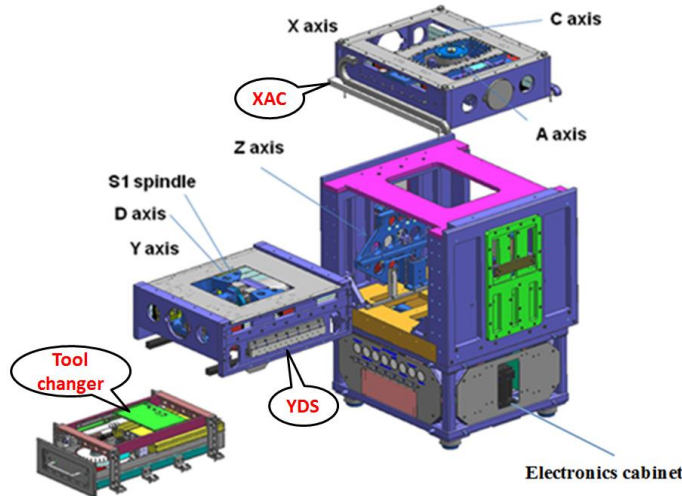


Figure 1: $\mu 4$ main sub modules

Only a limited range of materials been chosen for building precision machine tool structures: cast iron, granite or epoxy granite [2,3]. However, the $\mu 4$ structural material was chosen to be aluminium due to its low specific density which allows reducing the machine mass and size. Furthermore, choosing aluminium rather than steel was made due to its better thermal behaviour for steady heat flow and shorter settling time of a transient non uniform temperature distribution (Table 1). However, this comes at the expense of structural stiffness and dimensional stability for slowly fluctuating temperature. Stiffening the structure may reduce positional errors which determine the machine accuracy. However, positional errors can consist of up to 70% thermal derived errors [4]. By accurately modelling the machine, thermal errors can be minimised and compensated [5].

This article assesses the benefits and limitations of employing different materials to the machine structure by focusing on the thermal distortion of a linear motion system based on air bearing. Thus, the experiments and simulations were made on a linear motion system with a ‘bimetallic’ design.

2 Linear motion system

Figure 2 shows the YDS motion module prototype and its main components – frame, air-bearing and guideways, linear motor, and linear encoder. The frame is designed with four aluminium plates bolted together. In order to achieve high performance, the plates are diamond machined to assure precise assembly tolerances. The diamond machining reduces the thermal contact resistance across joints by increasing the area of contact.

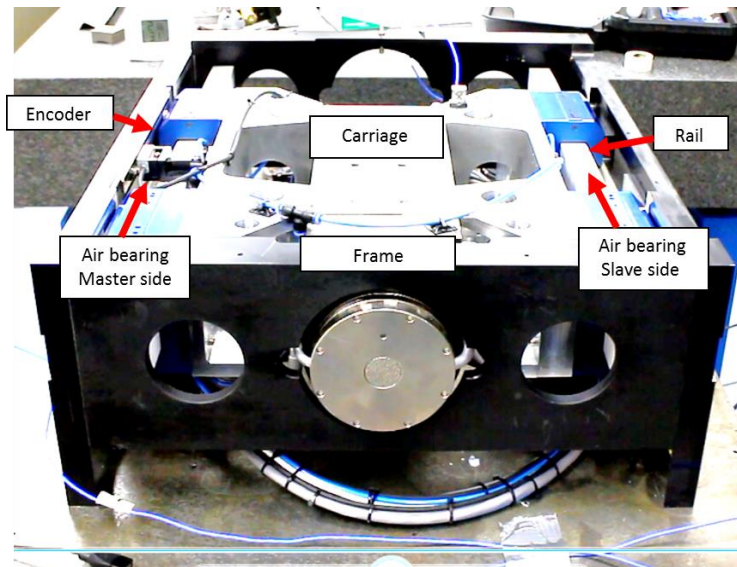


Figure 2: YDS motion module

The module is designed with master-slave bearing configuration (Figure 3), where in the master side there is the linear motor and linear encoder. In the master side, each bearing unit has 6 pads, while in the slave side there are only 2 pads (arrows, Figure 3) to give vertical restrict. The air bearing was designed with $3\mu\text{m}$ air gap which sets the limit for thermal distortion of the guideways. The guideways are fixed to the frame using bolts.

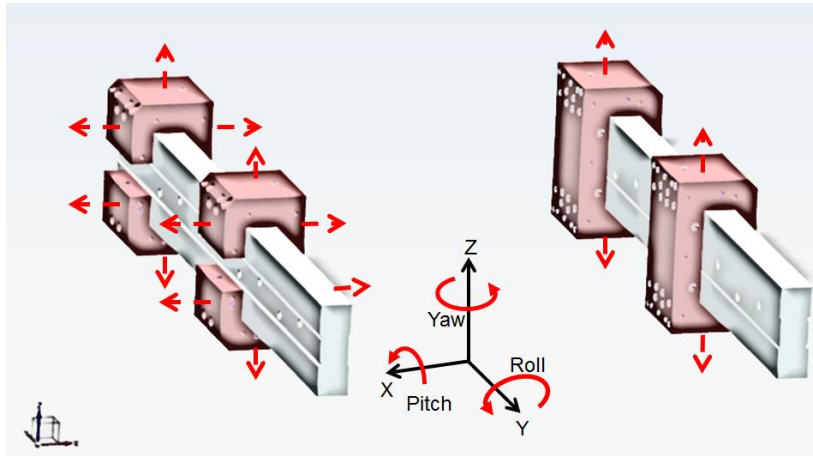


Figure 3: Air-bearing arrangement

In order to improve structural stiffness of the module, guideways made of alumina were considered. Alumina has higher specific stiffness and lower Coefficient of Thermal Expansion (CTE) than aluminium (Table 1). Consequently; stiffening of the structure comes at the expense of thermal distortion due to ‘bimetallic’ effect of the alumina-aluminium components.

Table 1: Material properties

	Aluminium 6061 ⁽¹⁾	AD 96 ⁽²⁾	Stainless steel 304 ⁽³⁾
$\rho \cdot E^{-1} [\text{s}^2 \cdot \text{m}^{-2}] \cdot 10^{-6}$	0.39	0.12	0.4
$\alpha \cdot \lambda^{-1} [\text{m} \cdot \text{W}^{-1}] \cdot 10^{-6}$	0.14	0.24	1
$\rho \cdot C_p \cdot \lambda^{-1} [\text{s} \cdot \text{m}^{-2}] \cdot 10^{-6}$	0.01	0.5	0.6
$\alpha [\mu\text{m}/\text{m} \cdot ^\circ\text{C}]$	23.6 @ 23-100 °C	6 @ 25-200 °C	17.3 @ 0-100 °C

E- Young modulus, ρ - density, α - CTE, λ - thermal conductivity, C_p - specific heat, ⁽¹⁾ [6,7], ⁽²⁾ supplier, ⁽³⁾ [6,7]

3 Methodology

In order to measure the thermal influence of the motion module, it was measured at different temperatures whilst mounted on a Coordinate Measuring Machine (CMM). The thermal measurements methodology is a bottom-up process with four sub-assembly levels (Figure 4). Individual components (the lowest level of sub-assembly) are tested and analysed first, then used to facilitate testing of higher sub-assemblies levels. The four sub-assembly levels are:

- Level A components only – guideway, restraint bar and frame plates
- Level B assembly of the guideway and restraint bar
- Level C assembly of frame plate and level B assembly

- Level D the full linear motion system assembly

The level A results were compared to the literature CTE values. Level B and C results were compared to Finite Element Modelling (FEM) results.

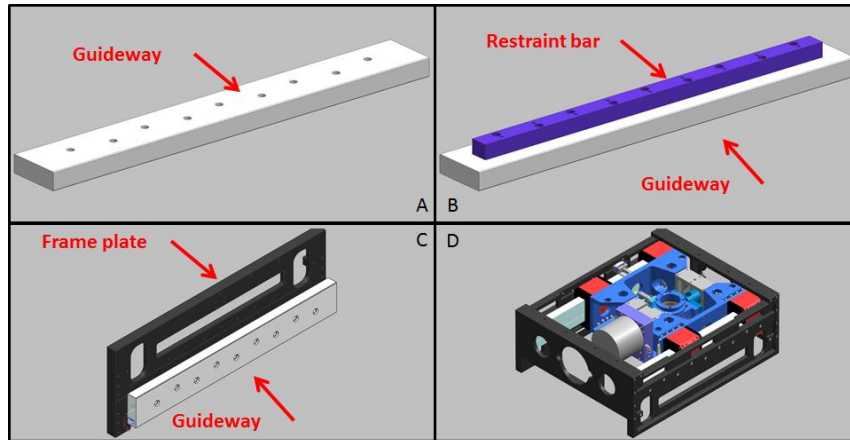


Figure 4: Bottom up thermal measurements

At each level the sub-assembly was supported on a three points posts mounted on the CMM (Figure 5). The Leitz PMMF CMM is equipped with low force sensing head with a traceable accuracy of $1.9 + (L/400) \mu m$ with an nm resolution. Sub-assemblies were heated by 10 °C. To achieve high signal to noise ratio of the measured distortion a significant elevated temperature was chosen. The component, CMM and the supporting posts temperatures were monitored at various points using K type thermocouples and data loggers. Heating the component was made by using Halogen light projectors as radiation heat sources. Thus, special care was made to heat only the components by applying insulation material which insulates the CMM from the “hot” components. Aluminium foil was used to reflect any stray light from the CMM (Figure 5).

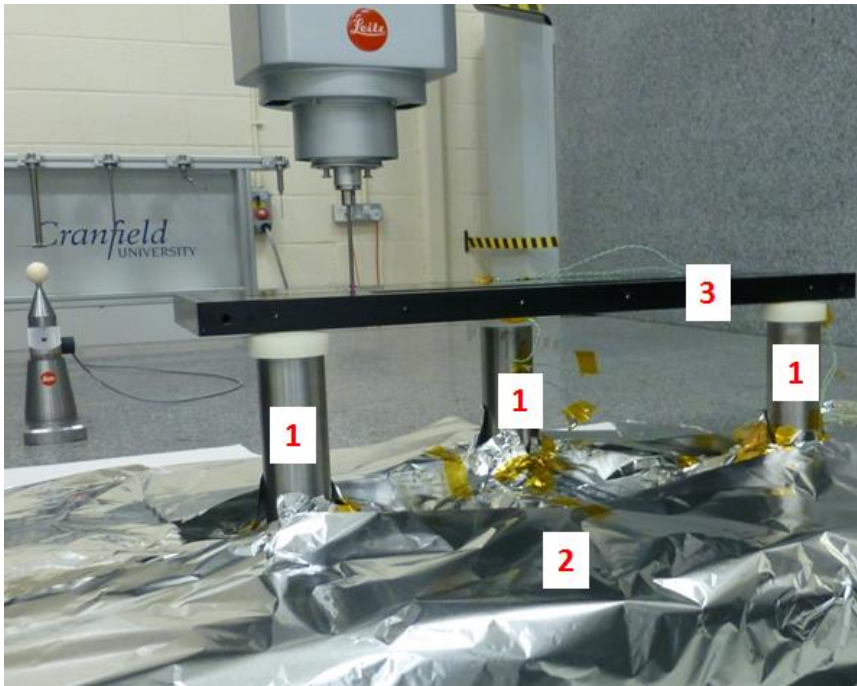


Figure 5: Measurement setup, (1) three points support post, (2) reflection and insulation materials and (3) measured component – frame plate

The thermal distortion assessed by measuring the sub-assembly at ambient temperature (reference measurement) and then repeating the same measurements at elevated temperatures. During each measurement, a uniform temperature distribution of the sub-assembly was monitored and confirmed to a ± 0.25 °C.

The important thermal distortion is of the guideways, since the motion is defined by the master and slave guideways.

4 Results

4.1 Level A measurements

The level A measurements allowed a comparison of the measured and published CTEs. This comparison was used to validate the setup – the thermocouples, CMM and supports.

The expected and measured phenomenon was a linear expansion without any distortion. The measured CTE was found to be 5.7 and 24.3 $\mu\text{m}/\text{m}\cdot^\circ\text{C}$ for the alumina and aluminium respectively. The measured CTE values show a maximum discrepancy of 5 %, which can be explained by measurements errors (temperature and CMM) and since that the theoretical CTEs are averaged over a

wide band of temperatures. Furthermore, CTE measurements are not better known than within $\pm 0.22 \cdot 10^{-6} \text{ K}^{-1}$ [8].

4.2 Level B and C measurements

Due to the bimetallic effect the assembly is expected to be bent. Hence, the deflection was calculated by subtracting the reference profile from the measured profile at elevated temperatures. Figure 6 shows the setup for sub-assembly level C (Figure 4 C). The deflection of upper surface (3A) is shown in Figure 7. Deflection occurred only on the Y axis since the CTE changes only on that axis.

At elevated temperatures the deflection has a convex profile, i.e., 28.19 °C. However, when the temperature returns to the ambient temperature, it changes to a concave profile i.e., 21.17 °C. This can be explained by hysteresis and due to the fact that only screws were used to connect components.

Due to the significant CTEs difference the level B and C sub-assemblies bends at a rate of $\sim 8 \mu\text{m}/^\circ\text{C}$ and $12 \mu\text{m}/^\circ\text{C}$ respectively.

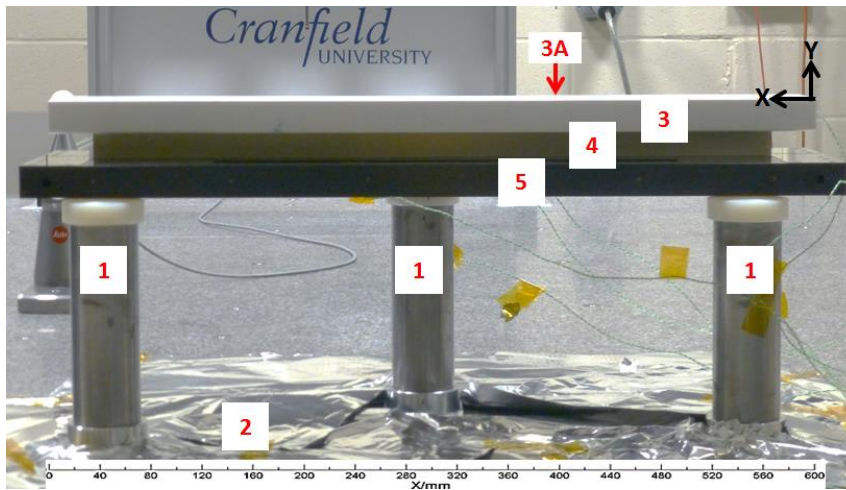


Figure 6: Level C assembly - (1) support post, (2) reflection material, (3) alumina guideway, (3A) guideway upper surface, (4) aluminium restraint bar, (5) aluminium frame plate

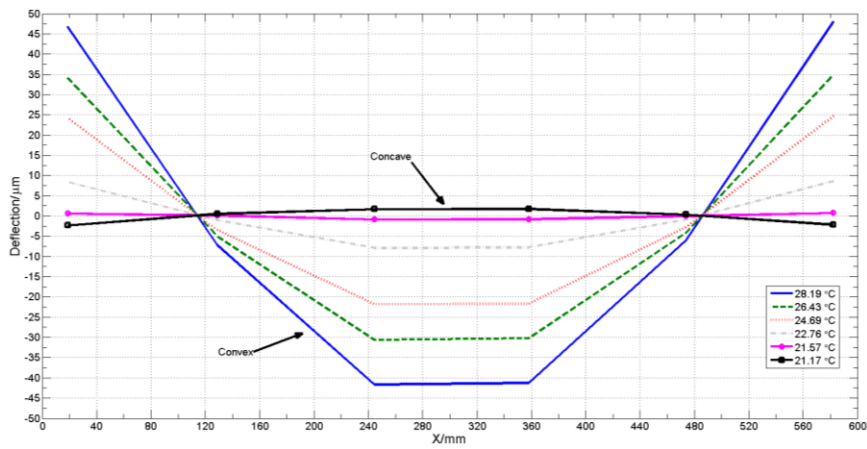


Figure 7: Level C assembly – guideway upper surface deflection

4.3 Level D measurements

Level D assembly (Figure 4 D) was measured using the same method as level C and B. Due to the fact that the carriage is thermally insulated from the guideway by air film, the temperature of the carriage itself and the air bearing were monitored too.

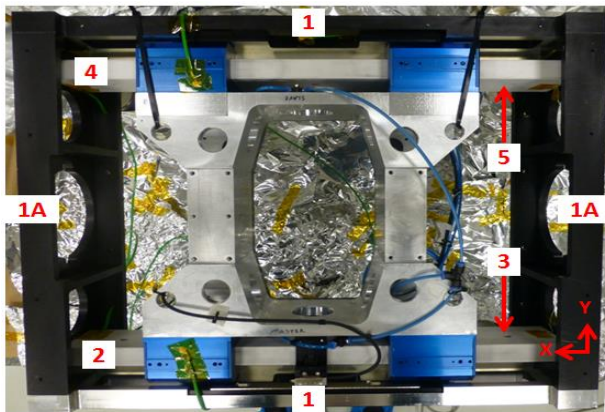


Figure 8: Level D assembly – (1) and (1A) aluminium frame plates, (2) and (3) master guideway top and side surfaces respectively and (4) and (5) slave guideway top and side surfaces respectively

The deflection in the Y axis is mainly important in the master side due to the air bearing design. However, comparing the deflection of both sides shows nearly symmetric results (Figure 9). The deflections in the master side show higher values than the slave side.

As in level B and C assemblies, while the temperature returns to the ambient temperature the deflection profile changes its sign.

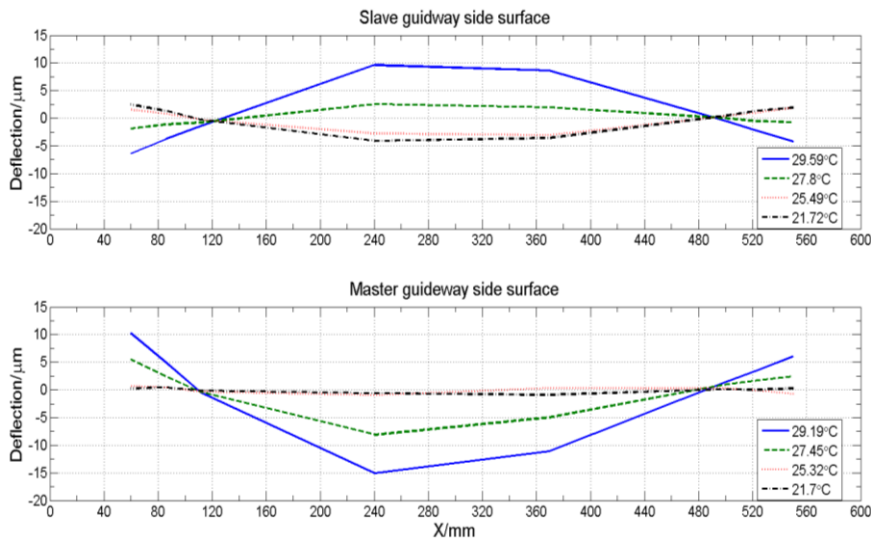


Figure 9: Level D assembly - master and slave guideways side surfaces deflections

4.4 FEM and measurements correlation

Figure 10 shows comparisons between FEM and deflections measurements of levels B and C. The three supporting points and the measured temperature (29.6 °C and 28.2 °C for level B and C respectively) were used as a boundary condition to the FEM simulation and the measured CTE was used as the material properties.

As shown, the higher level of the assembly the higher discrepancy between the simulations and measurements. This can be explained since that at higher level assembly there are more joints and interfaces which are hard to simulate. The maximum discrepancy is 6 % and 18 % for level B and level C respectively.

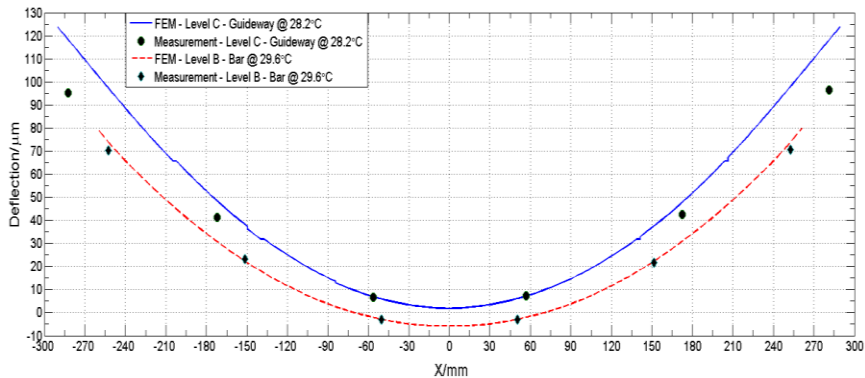


Figure 10 FEM and measurements correlations, the shown measured deflection is the aluminium bar and alumina guideway in level B and level C respectively

5 Conclusions and future work

The $\mu 4$ machine tool has a compact design. The design is based on aluminium as the main structural material due to its low density. Air bearings guideways were chosen to be made of alumina due to its high specific stiffness in order to stiffen the structure and to achieve high performances.

The thermal distortion was measured and simulated based on a “bottom up” methodology. It allowed analysing the influence of each joint to the deflection of the guideways. The measurements were made using a unique setup which allow heating and measuring the thermal distortion while the assembly mounted on a CMM.

The thermal distortion which affects the machine performances is the master side guideway. Thus, the dynamic performances are temperature dependant.

Comparing the deflection values shows that from level B to level C the deflection was increased. However, at level D the deflection was reduced significantly. The reason for that is that in level D the bending of the guideways is restrained by the frame due to its symmetric design. The restrained bending causes stress in the system, which is undesirable in bolted joints.

The proposed design requires a further improvements thus, a future work will include:

- Adding a flexure to the master side which will further reduce the deflection
- A casting design to allow buckling
- Dynamic performance measurements at ambient and elevated temperatures with the improved design

References

- (1) Design overview of the $\mu 4$ Compact 6 axes ultra precision diamond machining centre. 10th International Conference and Exhibition on Laser Metrology, Machine Tool, CMM & Robotic Performance. Buckinghamshire, UK: European Society for Precision Engineering & Nanotechnology; 2013.
- (2) Huo D, Cheng K, Wardle F. Design of a five-axis ultra-precision micro-milling machine UltraMill. Part 1: holistic design approach, design considerations and specifications. *The International Journal of Advanced Manufacturing Technology* 2010 04/01;47(9-12):867-877.
- (3) Luo X, Cheng K, Webb D, Wardle F. Design of ultraprecision machine tools with applications to manufacture of miniature and micro components. *J Mater Process Technol* 2005 8/30;167(2-3):515-528.
- (4) Ramesh R, Mannan MA, Poo AN. Error compensation in machine tools — a review: Part II: thermal errors. *Int J Mach Tools Manuf* 2000 7;40(9):1257-1284.
- (5) Ito Y. *Thermal deformation in machine tools*. : McGraw-Hill; 2010.
- (6) Kammer C. *Aluminium Handbook. I. Fundamentals and Materials*. 1999.
- (7) Smith ST. *Foundations of ultra-precision mechanism design*. : CRC Press; 2003.
- (8) James J, Spittle J, Brown S, Evans R. A review of measurement techniques for the thermal expansion coefficient of metals and alloys at elevated temperatures. *Measurement Science and Technology* 2001;12(3):R1.